Electronic Supplementary Material (ESI) for Lab on a Chip
This journal is © The Royal Society of Chemistry 2013

Electronic Supplementary Information (ESI)

Dynamic microbead arrays for biosensing applications

Mael Manesse, Aaron F. Phillips, Christopher N. LaFratta, Manuel A. Palacios, Ryan B. Hayman and David R. Walt*

Department of Chemistry, Tufts University, 62 Talbot Avenue, Medford, Massachusetts, USA.
*Corresponding author: Fax: 016176273443; Tel: 016176273470; E-mail: david.walt@tufts.edu

Contents:

This journal is © The Royal Society of Chemistry 2013

Nucleic acid sequences

Gene	Sense primer sequence	Anti-sense primer sequence	Capture probe Sequence	Amplicon length (bases)	*E. coli* strains
rfbE	TACTACAGGTGAAGGTGGAATG	GCTTGTTCTAACTGGGCTAATC	GGCATGACGTTATAGGCTACAATTATAGGA	177	43888,43889,43490, and 43894
stxI	AGAATGGCATCTGATGAGTTTCC	GCACTGAGAAGAAGAGACTGAAG	TATGTGTCAGGCAGATGGAAGA	329	43890 and 43894
stxII	ATGGAGTTCAGTGGTAATACAATG	ACAGGAGCAGTTTCAGACAG	TTACGCTTCAGGCAGATACAGAGAGAATTT	137	43889 and 43894

SI Table 1: Primer and capture probe sequences, product lengths and corresponding strains

Optical tweezers platform characterization

An easy way to characterize the trapping efficiency of an optical tweezers system is to determine its Q value (Equation 1), a dimensionless parameter proportional to the ratio of the force applied to a particle F_{op} over the optical power used to exert this force.

Equation1:

$$Q = \frac{F_{\text{op}}\, c}{nP} \qquad F_{\text{op}} \approx F_{\text{Stokes}}$$

Where Q is the parameter describing the trapping efficiency, F_{op} the optical force exerted on a particle, c the speed of light, n the refractive index of the medium, and P the power of the trapping laser. F_{op} can be measured by applying another increasing force until the particle falls out of the trap. At this point, the two forces are equal. Here we apply a lateral drag force, known as the Stokes force, by translating the motorized stage at a constant velocity while a bead is optically trapped. The expression of the Stokes force with Faxén's law correction to take into consideration the interaction between the trapped particle and the surface of the coverslip is given by Equation 2.

Equation 2:

$$F_{\text{Stokes}} = \frac{6\pi\eta r v}{1 - \frac{9}{16}\left(\frac{r}{h}\right) + \frac{1}{8}\left(\frac{r}{h}\right)^3 - \frac{45}{256}\left(\frac{r}{h}\right)^4 - \frac{1}{16}\left(\frac{r}{h}\right)^5}$$

The drag force exerted on the bead depends on the dynamic viscosity η of the medium containing the particle, the radius r of the particle, the velocity v at which the particle is travelling, and the distance h between the particle and the surface of the coverslip. The Stokes force corresponding to the optical force can be calculated using the measured velocity when the particle falls out of the trap.

The optical force exerted by the optical tweezers setup on a bead was measured for different sizes of trap arrays. In order to keep the hydrodynamic properties constant, the experiments were conducted with a single bead trapped. For example, the scanning mirrors were configured to create a 4×4 array, but only one bead was trapped in the array. This ensures that the average "on" time corresponds to the size of the array studied. Trapping more than one bead could lead to a shielding effect between the beads, reducing the drag force applied to the particles, especially in the central positions of the array. As expected, as the size of the trap array increases, the average optical force exerted on the particles decreases, because the average time each bead is illuminated decreases (SI Fig. 1). The time-averaged optical power delivered to each bead every second can be calculated using the "on" times for each array size. The linear evolution of the optical force with the time-averaged laser power is shown in the insert of SI Fig. 1. According to Equation 1, Q can be calculated using the slope of the curve and is equal to 0.114.

This journal is © The Royal Society of Chemistry 2013

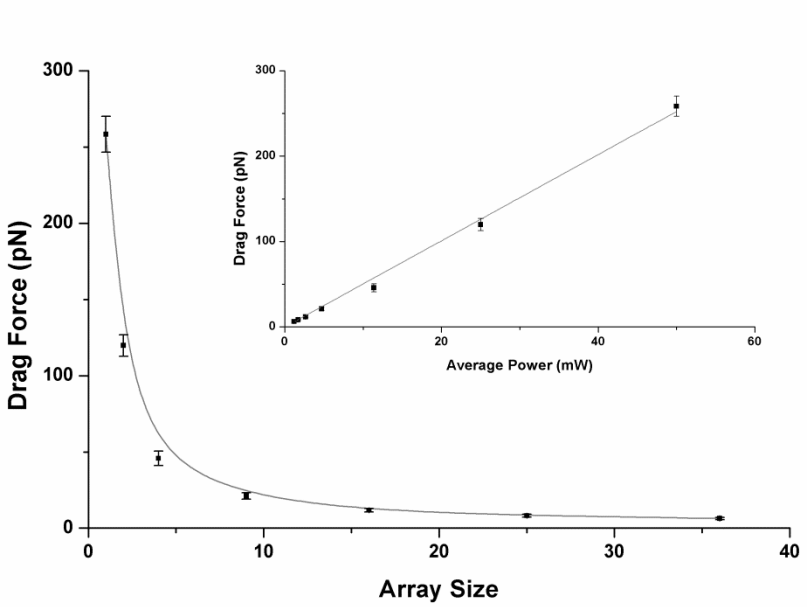

SI Fig. 1: Evolution of the measured drag force with the size of the optically trapped array of beads. The insert shows the linear relation between the drag force and the average laser power calculated from the time each bead is illuminated.

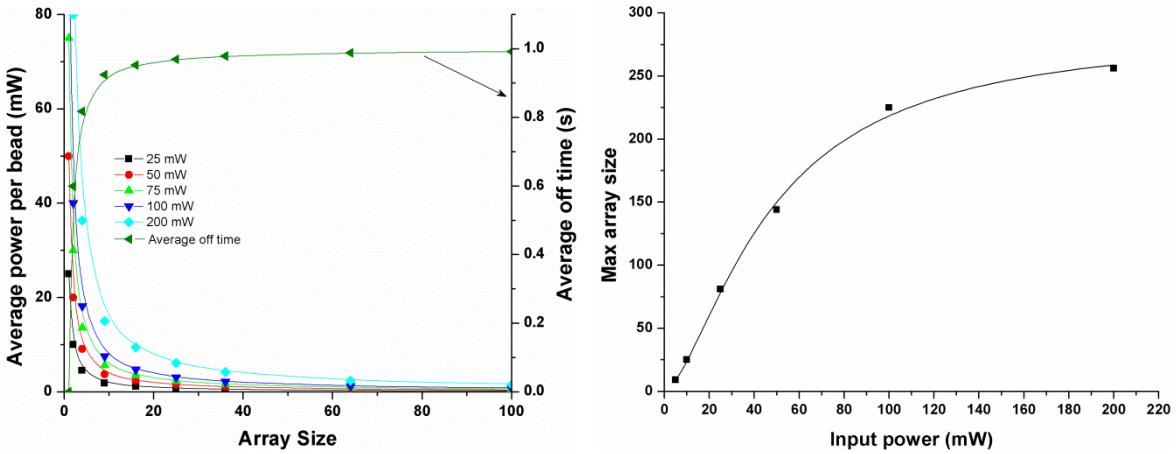

SI Fig. 2 a: Evolution of the time-averaged power delivered to each bead as a function of array size. Black squares, red circles, green upward triangles, blue downward triangles, and cyan diamonds correspond to input powers of 25, 50, 75, 100, and 200 mW respectively. Evolution of the average off time with increasing array sizes (dark green triangles). b: Evolution of the maximum array size with increasing input power.

As the number of trapping positions in the array increases, the "off" time at each position increases (SI Fig. 2a dark green), and the average "on" time decreases. As a result, the time-averaged power at each position decreases quickly (SI Fig. 2a). To balance this effect, the power of the trapping source can be increased (black, red, green, blue, and cyan lines on SI Fig. 2a), allowing larger arrays to be assembled (Fig. 2b). However, because the time-averaged power decreases sharply with the number of trapping positions, the input power necessary to trap large arrays can become very high. SI Fig. 2b presents the evolution of the maximum array size obtained with increasing input power. The maximum array size increases linearly with the input power, up to 50 mW, then reaches a plateau for higher array sizes. The linear part of the curve presents a slope of 3 beads per mW of input power. The plateau is mostly due to the effects of longer off times, which allow the beads to diffuse from their position. For example, a bead

This journal is © The Royal Society of Chemistry 2013

is irradiated by the trapping source every 60 ms in a 15×15 array. This long off time results in a limit of the maximum array size.

Quantum dots spectral characterization

Quantum dots present many advantages for the development of multiplexed assays: they offer a narrow emission peak, a strong resistance to photobleaching, high quantum efficiency, and a broad excitation spectrum which leads to single wavelength excitation.

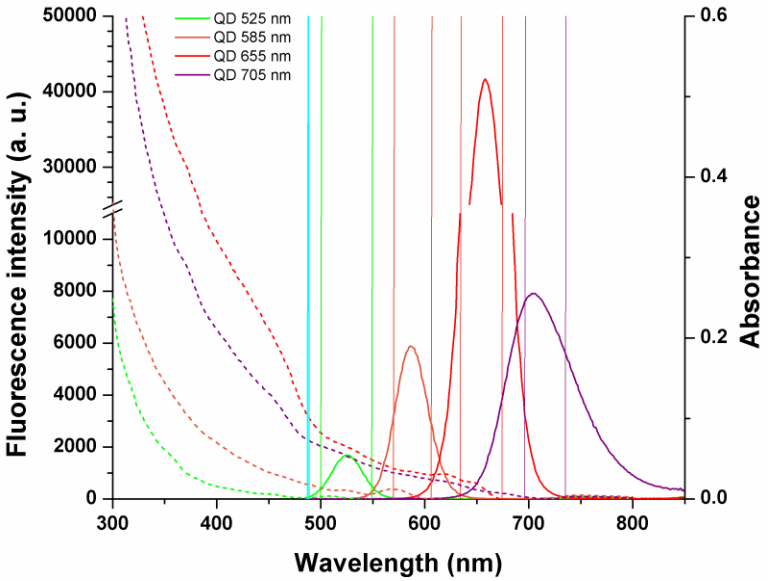

SI Fig. 3: Fluorescence emission spectra for the four different types of QDs (solid lines). Green, orange, red and violet lines correspond respectively to the QDs dots emitting at 525, 585, 655 and 705 nm, at a concentration of 40 nM in water. The excitation light was set at 488 nm. The dashed lines correspond to the absorbance spectra. The vertical cyan line represents the excitation laser. The bandwidth for the different emission filters is represented by the vertical lines. Green, orange, red, and violet correspond to the bandwidths centered at 525, 587, 655, and 716 nm respectively.

SI Fig.3 shows the absorption and emission spectra for the QDs emitting at 525, 585, 655 and 705 nm. The vertical bars (green, orange, red, and violet) represent the filters' bandwidths used in our system, centered at 525, 587, 655, and 716 nm respectively. The filters were chosen to limit the effect of spectral overlap between the different QDs, in particular between the QDs emitting at 655 and 705 nm.

Primers evaluation

After amplification, the results of the PCR were evaluated using gel electrophoresis (SI Fig. 4). For reference, the *rfbE* gene is expressed by the four studied strains, and the amplicon appears as a band in the lanes 5, 6, 7, and 8 (amplicon size 177 base pairs). The *stxI* gene is only present in the 43890 and 43894 strains, and the band corresponding to the amplicon (349 base pairs) appears in lanes 7 and 8. The *stxII* gene is expressed by the strains 43889 and 43894, and the amplicon appears as a band in lanes 6 and 8.

This journal is © The Royal Society of Chemistry 2013

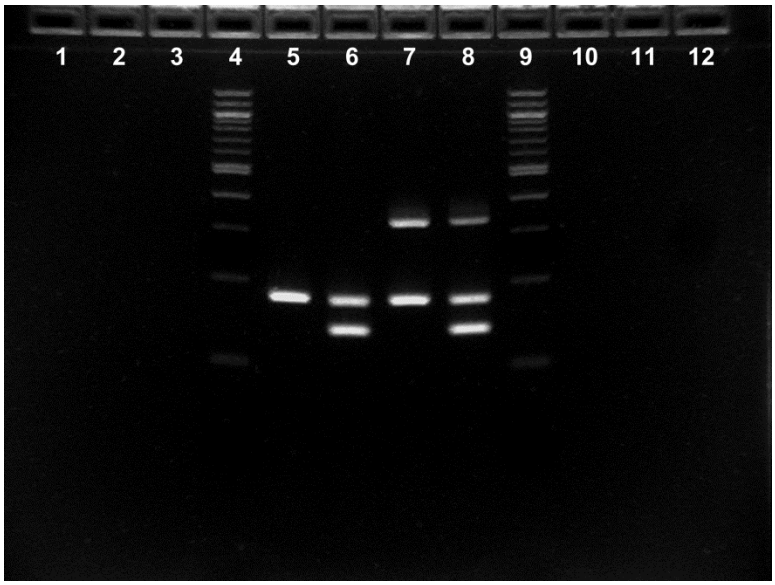

SI Fig. 4: Fluorescence image of an electrophoresis gel with the results of the PCR using the designed primers (for the *rfbE*, *stxI*, and *stxII* genes) and DNA templates from live E. coli cells. The strains used were ATCC# 43888, 43889, 43890, and 43894, corresponding to lanes 5, 6, 7, and 8 respectively. A DNA ladder (100 base pairs) was added in lanes 4 and 9.